2011 IEEE International Conference on Rehabilitation Robotics
Rehab Week Zurich, ETH Zurich Science City, Switzerland, June 29 - July 1, 2011

Model Predictive Control-based Gait Pattern Generation for Wearable Exoskeletons

Letian Wang, Edwin H. F. van Asseldonk
Laboratory of Biomechanical Engineering
University of Twente
7500 EA Enschede, the Netherlands
letian.wang@utwente.nl

Herman van der Kooij
Biomechatronics and Rehabilitation Technology
University of Twente
Enschede, the Netherlands
Biomechanical Engineering Dept.
Delft University of Technology,
Delft, the Netherlands
h.vanderkooij@utwente.nl

***Abstract* — This paper introduces a new method for controlling wearable exoskeletons that do not need predefined joint trajectories. Instead, it only needs basic gait descriptors such as step length, swing duration, and walking speed. End point Model Predictive Control (MPC) is used to generate the online joint trajectories based on these gait parameters. Real-time ability and control performance of the method during the swing phase of gait cycle is studied in this paper. Experiments are performed by helping a human subject swing his leg with different patterns in the LOPES gait trainer. Results show that the method is able to assist subjects to make steps with different step length and step duration without predefined joint trajectories and is fast enough for real-time implementation. Future study of the method will focus on controlling the exoskeletons in the entire gait cycle.**

Keywords-wearable exoskeleton, gait cycle reference, end point control, model predictive control

I. INTRODUCTION

An increasing number of wearable exoskeletons and robotic gait training devices are used in physical gait training for patients with walking difficulties after neurologic injuries such as stroke or spinal cord injury. Control algorithms for these exoskeletons and robots are designed to support the patient (when needed). A recent review [1] showed that most robots are currently controlled by using reference trajectories that are defined for the complete gait cycle. This control is implemented for Lokomat [2], LOPES [3], Active Leg Exoskeleton (ALEX) [4], Gait Trainer [5], and Ankle Robot for modular gait rehabilitation [6]. This kind of control enables a full realization of the assistive and challenge-based therapies that dominate in the current robotic therapies [1].

The reference gait trajectory-based control scheme requires a detailed specification of the gait pattern. A typical trajectory consists of joint angles and velocities of the lower limb as functions of the percentage of the gait cycle. Generally there are two methods to define such trajectories.

1. Predefine a trajectory according to normal gait. The predefined trajectory includes joint angles derived from mathematical models of normative gait trajectories [7, 8] or imitated from prerecorded gait trajectories of healthy subjects [9, 10].
2. Define an instant trajectory from the unimpaired lower limb. Motions of the unimpaired lower limb are detected and dynamically mapped to the reference trajectory of the other limb using complementary limb motion estimation (CLME) [11] or Central Pattern Generators (CPG) [12].

The gait pattern of the trajectory specified by the first method is non-adaptive because it is not possible to smoothly transfer from one gait pattern to another. The second method has good performance but can only be applied to the gait therapy consisting of bilateral tasks. Moreover, both methods are not suited for controlling assistive devices as they are not able to cope correctly with external perturbations. It is well known that, to maintain balance in case of external perturbations, one must appropriately adjust his foot placement. The reference trajectory-based methods cannot easily realize such adaptation to step length and width during walking. So they cannot ensure body stability for the exoskeletons that do not assist body stability (often seen in mobile wearable exoskeletons [13, 14]).

Van der Kooij et al. showed that, using end point Model Predictive Control (MPC), it is possible to generate gait trajectory in real time, which leads to stable gait for biped robots based on simple gait descriptors such as step length, step duration, and walking speed [15]. Thus, this method can easily collaborate with balance control schemes such as extrapolated center of mass (XCoM) [16] to place the foot where the balance controller suggests.

Instead of using end point MPC in the control of biped robots, it might also be applicable in the control of assistive robotics. However, a main obstacle toward implementation is the large computation times [17]. This is because the end point MPC requires considerable time to deduct the linearization and prediction. With the advent of faster computer processors (see Moore's Law), the problem of computation time becomes less crucial compared with six or seven years ago. Faster and more efficient Model Predictive Control algorithms [18-20] haven been published and implemented in fast systems [21].

The research is sponsored by MINDWALKER project funded under the Seventh Framework Programme of European Commission. The contact number is FP7-ICT-2009.7.2 #247959.

978-1-4244-9862-8/11/$26.00 ©2011 IEEE

The goal of this paper is to demonstrate the feasibility of the end point MPC control scheme in powered lower extremity exoskeletons.

II. Method

A. Models of the Exoskeleton and Human

The exoskeleton model for the MPC controller was derived from the LOPES exoskeleton [3]. Each limb of the LOPES consists of a thigh and shank and was modeled as a double pendulum (DP) (Fig. 1). A first test of the end-point MPC control scheme was to let the wearable exoskeleton make a step. We only considered the swing phase of one limb during walking in anterior–posterior (sagittal) plane. Thus, two degrees of freedom (DoFs) of motion were controlled, namely hip flexion and knee flexion. They were defined as,

$$q = \begin{bmatrix} \theta_1 \\ \theta_2 \end{bmatrix} \tag{1}$$

where θ_1 is the hip angle and θ_2 is the knee angle. The two joints were driven by series elastic actuators.

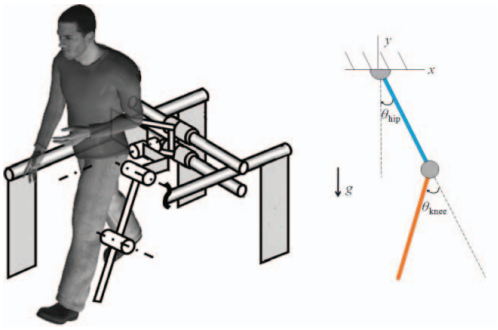

Fig. 1. LOPES exoskeleton (left), double pendulum in sagittal plane (right). Each limb of the LOPES consists of a thigh and a shank. The two-segment linkage was modeled as a double pendulum.

The equations of motion in sagittal plane were derived following Lagrangian formalism, and are given by:

$$M(q)\ddot{q} = G(q) + C(q,\dot{q}) + Bu \tag{2}$$

where $\boldsymbol{M}$ is the mass matrix and $\boldsymbol{G}$ is the gravitational matrix (including spring constants). $\boldsymbol{C}$ defines the centripetal and coriolis forces (including damper constants) and $\boldsymbol{B}$ denotes the vector with external perturbations and joint torques.

The human leg in the LOPES exoskeleton was modeled by its mass and inertia [22]. The stiffness and damping of the hip and knee joints were neglected for this experiment.

B. General Control Scheme

The general idea of the control was to drive the exoskeleton from an initial position to a desired position within certain duration. The desired position was expressed by the gait descriptors specified by high-level controllers such as balance controllers. The MPC controller calculated a proper gait trajectory to connect the two positions based on the prediction output from the exoskeleton and human model. The general control scheme of the proposed method is shown in Fig. 2. The controlled variables are the joint angles and the control variables are the joint torques.

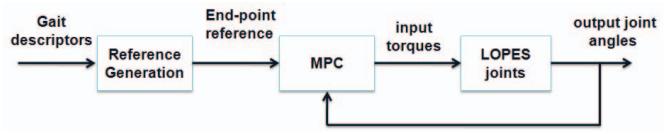

Fig. 2. The block diagram of the end point MPC control scheme.

The controller combines feedfoward with feedback control. The inputs are the gait descriptors (walking speed V, duration of the swing phase T, and step length S). The reference generation block transfers these descriptors into end-point references. The end-point reference is the reference that should be reached only at the end of the control horizon (i.e. end of the swing phase). At the beginning of the swing phase, the joint positions of the hip and knee are known as the initial condition. The joint positions of the hip and knee at the end of the swing phase can be calculated geometrically given either two of the three descriptors V, S or T (Fig. 3). These end-phase joint positions are set as the end-point reference fed to the MPC controller. The MPC controller will compute the torques applied at each joint and the actual joint angles and velocities are fed back to the controller.

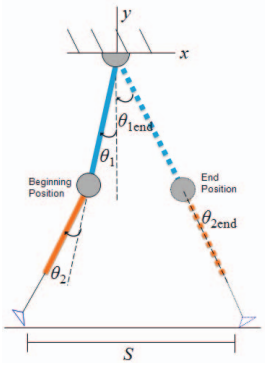

Fig. 3. Illustration of the end-point reference. It shows the position of one leg at different time spot, the beginning position with solid lines, the end position with dashed lines.

C. End point MPC controller

The function of the end-point controller is to let the joints reach the end positions at $t_{end}=t_0+T$ from the beginning positions at $t=t_0$ where T is the swing duration. The principle is shown in Fig. 4. The MPC employs a discrete Linear Time Invariant (LTI) model as the inner model. In our case, the LOPES and human model was linearized around its set point. The model inputs were joint torques $\boldsymbol{u} = [\tau_{hip} \quad \tau_{knee}]^T$ and the model outputs were joint angles and joint velocities $\boldsymbol{y} = [\theta_{hip} \quad \dot{\theta}_{hip} \quad \theta_{knee} \quad \dot{\theta}_{knee}]^T$. The bolded symbol stands for vector in this paper.

For every discrete time step k, the current plant input $\boldsymbol{u(k)}$ and output $\boldsymbol{y(k)}$ are fed back to the controller and a cost-minimizing control strategy (joint torques in our case) is computed for a discrete time period in the future: [k+1,

k+$P(k)$]. $P(k)$ is the prediction horizon at the current discrete time step k. Different from a standard MPC algorithm with a

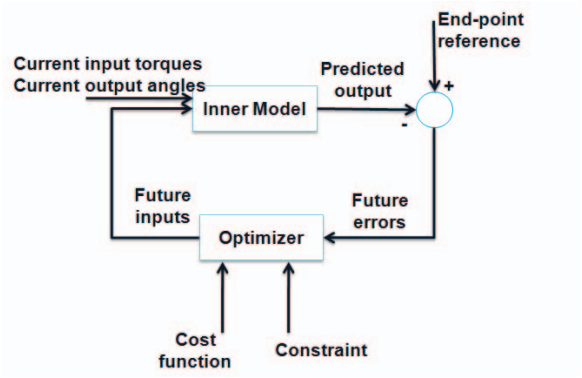

Fig. 4. The block diagram of the MPC controller.

fixed prediction horizon, our P is dynamic and is defined as:

$$P(k) = (t_{end} - t_{curr}) / Ts \tag{3}$$

where t_{curr} is the current time and Ts is the sampling time. At the first time step k=k_0 (t_{curr}=t_0), we have the largest prediction horizon P defined by $P_{\max}$:

$$P_{\max} = P(k_0) = T / Ts \tag{4}$$

where T is the swing duration. We also define a constant minimal prediction horizon:

$$P_{\min} = P(k_{end} - 4) = 4 \tag{5}$$

k_{end} is the last time step when t_{curr}=t_{end}. Then we have

$$P(k) = P_{\min} \quad \text{if} \quad k \geq k_{end} - 4 \tag{6}$$

The optimization calculates the torques for the whole prediction horizon but only the torques for the next time step k+1 are applied to the plant. Constraints on input torques τ (Nm) and output joint angles θ (degree) for the whole prediction horizon were specified as:

$$\begin{aligned} -80 \leq \tau_{hip} \leq 80 \\ -80 \leq \tau_{knee} \leq 80 \\ -90 \leq \theta_{hip} \leq 90 \\ 0 \leq \theta_{knee} \leq 90 \end{aligned} \tag{7}$$

No constraints were set to joint velocities at both hip and knee. The cost function to be minimized at the current step k is defined as:

$$\min_{\Delta u_i(k)} J = \sum_{i=1}^{N} \boldsymbol{\omega}_{y_i}(\boldsymbol{k})(\boldsymbol{r}_i(\boldsymbol{k}) - \boldsymbol{y}_i(\boldsymbol{k}))^2 + \sum_{i=1}^{M} \boldsymbol{\omega}_{u_i}(\boldsymbol{k})\Delta \boldsymbol{u}_i(\boldsymbol{k})^2 \tag{8}$$

where $k = [k+1, k+2, ..., k+P(k)]^T$. $\boldsymbol{r_i(k)}$ is the end-point reference for the i-th output. $\boldsymbol{y_i(k)}$ is the i-th output estimated by the inner model. $\boldsymbol{\Delta u_i(k)}$ is the i-th input changes defined as $\Delta u_i(k) = u_i(k) - u_i(k-1)$. N and M are the dimension of the input and output respectively. $\boldsymbol{\omega(k)}$ is the weight factor. It reflects the importance of the weighted content. To realize the end-point control, zeros are assigned to $\omega(k+1)$, $\omega(k+2)$,…, $\omega(k+P(k)-4)$ and positive scalars are assigned to $\omega(k+P(k)-3)$, $\omega(k+P(k)-2)$, $\omega(k+P(k)-1)$, $\omega(k+P(k))$ for the end objectives. In this paper, the positive scalar weights were set larger on hip joint angles than on the knee angles because hip angle error has larger influence on step length which is crucial for gait stability. The non-zero positive weights γ were set as:

$$\begin{aligned} &\left[\gamma_{\theta_{hip}} \quad \gamma_{\dot{\theta}_{hip}} \quad \gamma_{\theta_{knee}} \quad \gamma_{\dot{\theta}_{knee}} \quad \gamma_{\Delta\tau_{hip}} \quad \gamma_{\Delta\tau_{knee}}\right]^T \\ &= \left[25 \quad 2 \quad 10 \quad 2 \quad 0.2 \quad 0.2\right]^T \end{aligned} \tag{9}$$

At the last time step k_{end} (t_{curr}=t_{end}), the joint angles are supposed to reach the end positions. If so, the calculation iterations will be initialized for the next gait phase. Particularly in this paper, only one gait phase (the swing phase) was controlled. The joint positions were controlled to stay at the end positions when reaching there. If not, the iteration will not be initialized. The time steps will continue to count until the end positions are reached.

D. Implementation

The end-point MPC control algorithm with simple gait descriptors was implemented in the LOPES exoskeleton. The real time system and control software we used was Matlab Xpc and Simulink. The sampling frequency of the MPC controller was 50 Hz while the sampling frequency of rest of the control loop was 1000 Hz.

For variation in gait speed and for appropriate balance, it is important that one can make steps with different lengths and with different swing durations. Therefore, the experiment was designed to verify whether we could make such steps. As a preliminary exploration of the method, we only focused on the swing phase rather than on the entire gait cycle. Thus, we only tested the swing phase in this experiment.

The experiment was designed to swing one leg from a beginning position to an end position with different step lengths and swing durations in the LOPES exoskeleton. The beginning position was the toe-off of the swing leg and was kept constant. The end position was the heel-strike of the swing leg and it varied according to different step gait descriptors (walking speed V, step length S, or step time T). Although we performed the swing phase instead of the entire gait cycle, the walking speed could still be computed based on the assumption that the duration of double stand phase T_{sd} is a constant (10 percent of the swing phase) if the walking speed varies in a small range. The relationship among the three descriptors (S, T, V) is given by:

$$V = S / (T + T_{sd}) \ . \tag{9}$$

A healthy subject participated in the experiment. The subject stood on a stepping-stone with one foot and the other leg was attached to the LOPES (Fig. 5) so that the attached leg could swing freely. The subject was required to react passively in the exoskeleton to simulate the passive leg. One simulation and two experiments were performed. The simulation was carried out by swinging the exoskeleton model without human subject model attached. The aim is to test the control

performance in ideal conditions. The two experiments were carried out with and without a human subject attached in the exoskeleton respectively. In this way, we could explore the human influence on the control performance. For each simulation or experiment, eight trials were performed. Four trials had the same desired swing duration T=0.6 s while the step length S varied from 0.6 m to 0.9 m with 0.1 m interval. The other four trials have the same desired step length S=0.7 m while the desired swing duration varied from 0.5 s to 0.8 s with 0.1 s interval.

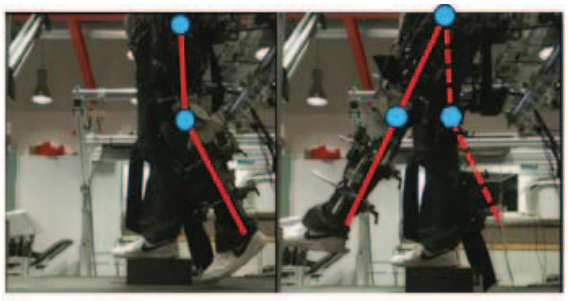

Fig. 5 Leg swing test in the LOPES exoskeleton, beginning position (left), end position (right).

III. Results and Discussion

A. Results

Simulation

The corresponding joint trajectories and actuation torques of hip and knee are shown in Figs. 6 and Fig. 7. If the actual joint angles reach the reference within the swing time T and stay there, we consider it a good tracking. The simulation results suggest the targets were all reached on time. Increasing the step length or decreasing swing duration, we can observe a linear increase on joint torques, which is a logical result of linear MPC (left plots Figs. 6 and 7). Peaks in knee angles indicate that knee flexion was present although no knee flexion reference was defined (Top right Figs. 6 and 7).

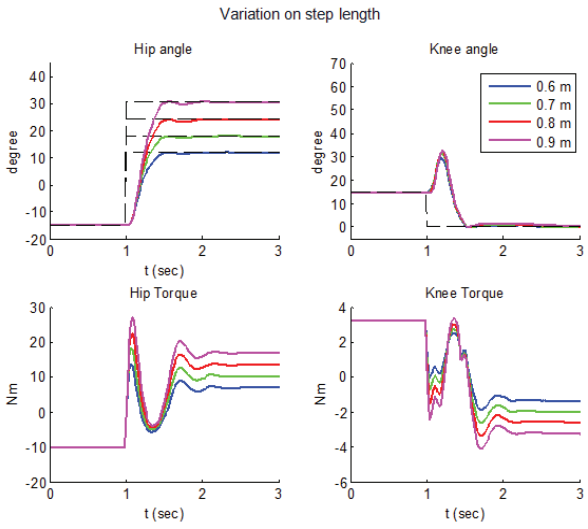

Fig. 6. Simulation without human: Joint trajectories and actuation torques of hip and knee for different desired step length given the desired step time 0.6 s. The black dashed lines are the reference.

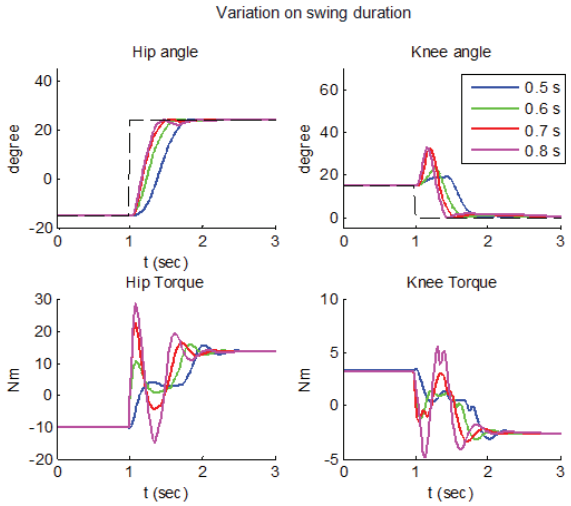

Fig. 7. Simulation without human: Joint trajectories and actuation torques of hip and knee for different desired walking speed given the desired step length 0.7 m. The black dashed lines are the reference.

Experiment without human

The corresponding joint trajectories and actuation torques of hip and knee are shown in Fig. 8 andFig. 9. The results suggest that the targets were all reached with a certain amount of delays (Tables 1 and 2). Knee flexion is hardly seen in knee angles (top right, Figs. 8 and 9). The patterns of the applied torques are similar among the trials and the amplitudes are proportional.

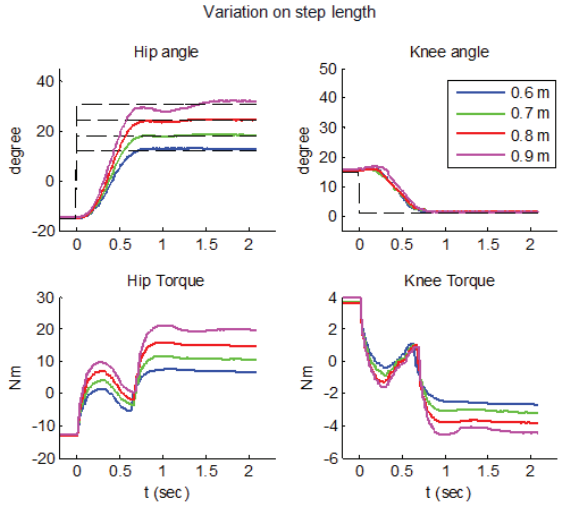

Fig. 8 Experiment without human: Joint trajectories and actuation torques of hip and knee for different desired step length given the desired step time 0.6 s. The black dashed lines are the reference.

Experiment with human

The corresponding joint trajectories and actuation torques of hip and knee are shown in Fig. 10 and Fig. 11. Although all targets were reached, the actual positions of hip angles have some vibrations after getting to the end positions. Larger delays can be found compared to results from the simulation and experiment without human (Tables 1 and 2). Irregular knee flexion was present during the swing (Top right Figs. 10 and 11). The applied torques didn't change linearly as we saw

in the previous experiments. We could find considerable vibrations in the torques during the swing (bottom plots Figs. 10 and 11). This suggests a certain amount of disturbance was introduced by the human subject during the leg swing.

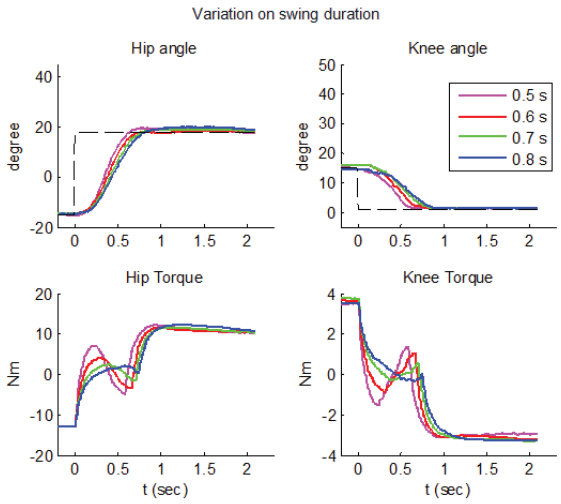

Fig. 9 Experiment without human: Joint trajectories and actuation torques of hip and knee for different desired walking speeds given the desired step length 0.7 m. The black dashed lines are the reference.

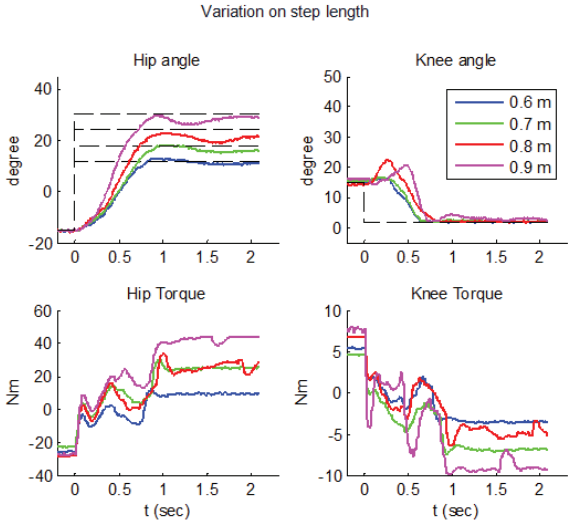

Fig. 10 Experiment with human: Joint trajectories and actuation torques of hip and knee for different desired step length given the desired step time 0.6 s. The black dashed lines are the reference.

The desired and actual swing durations for the simulation and two experiments are listed in Table 1, Table **2** because they are not clear in the above figures. The actual swing times were defined as the time at which hip joint angles reached their references (2 percent tolerance). If the actual swing duration T is equal to or smaller than the desired one, we consider it a good tracking.

B. Discussions

The goal of the experiment is to demonstrate that the proposed Model Predictive Control method can assist subjects to make steps in the exoskeleton. The results of the simulation

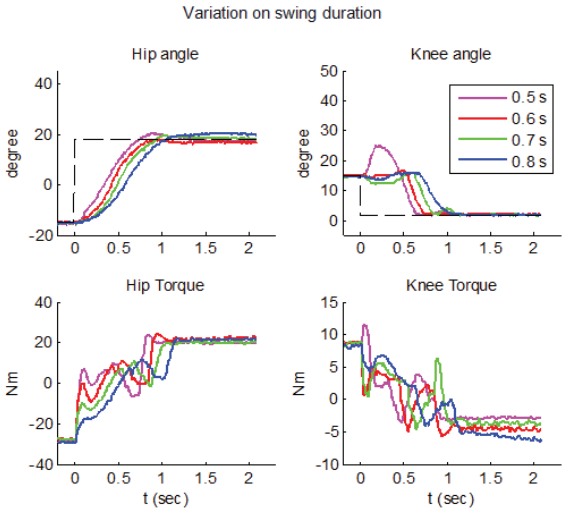

Fig. 11 Experiment with human: Joint trajectories and actuation torques of hip and knee for different desired walking speeds given the desired step length 0.7 m. The black dashed lines are the reference.

Table 1. The desired and actual swing durations at different step lengths based on the hip angles

Desired S (m)	**Desired T (s)**	**Actual T (s)**		
		Simulation	**Experiment without human**	**Experiment with human**
0.6	0.6	0.53	0.70	0.76
0.7	0.6	0.55	0.71	0.81
0.8	0.6	0.55	0.71	0.90
0.9	0.6	0.55	0.73	0.82

Table 2. The desired and actual swing times at different swing durations based on the hip angles

Desired S (m)	**Desired T (s)**	**Actual T (s)**		
		Simulation	**Experiment without human**	**Experiment with human**
0.7	0.5	0.45	0.61	0.73
0.7	0.6	0.55	0.71	0.81
0.7	0.7	0.64	0.75	0.90
0.7	0.8	0.81	0.80	1.02

and experiments showed the desired end positions of all the trials were reached, which suggests that the exoskeleton can make appropriate steps with different characteristics given simple gait descriptors in real time. However, the results from experiments were not as good as those from the simulation. This is because two problems that deteriorate the control performance were found in the experiments' results:

1. Time delay to reach the reference. In the ballistic walking, the time delay in reaching the end position will cause shorter-than-desired steps that lead to balance loss.

2. Insufficient or irregular knee flexion during the leg swing. An insufficient knee flexion will cause a stumble during walking.

From the comparison between the simulation and the experiments, we can conclude that the time delay and the insufficient knee flexion were mainly caused by deviations between the real system and ideal systems.

Several assumptions led to model error during the modeling of the LOPES and human system. First, the LOPES model was assumed to have very small frictions that could be neglected. The actual LOPES has approximately 2-3 Nm dynamic friction torques at each joint. The knee flexion was suppressed by this friction. Second, we assumed humans acted passively during the leg swing. However, it is impossible to react passively in reality. The considerable variations in the applied torques in the experiment with human indicate that the MPC rejected the disturbance from the human subject but not completely.

The control performance can possibly be improved by updating the model through online identification of human limb dynamics. Once a sufficient and accurate control of the swing phase is achieved, the control algorithm will be extended to control the entire gait cycle.

IV. CONCLUSION

This paper presented an alternative control method for generating gait patterns for wearable exoskeletons. Instead of defining the whole gait cycle references, it only defines some key gait parameters. A Model Predictive Control method was used to generate online gait trajectories based on the key gait parameters. The results showed that the proposed method can assist subjects in making appropriate steps with different characteristics given simple gait descriptors in real time. The performance of the method could be enhanced by improving the model of the human leg and the exoskeleton.

V. ACKNOWLEDGMENTS

The authors would like thank B. Koopman for his contribution to the research. The work was part of the MINDWALKER project funded under the Seventh Framework Programme of European Commission. The contact number is FP7-ICT-2009.7.2 #247959.

REFERENCE

1. Marchal-Crespo, L. and D. Reinkensmeyer, *Review of control strategies for robotic movement training after neurologic injury*. Journal of NeuroEngineering and Rehabilitation, 2009. **6**(1): p. 20.
2. Colombo, G., et al., *Treadmill training of paraplegic patients using a robotic orthosis*. Journal of Rehabilitation Research and Development, 2000. **37**(6): p. 693-700.
3. Veneman, J., et al., *Design and evaluation of the LOPES exoskeleton robot for interactive gait rehabilitation.* IEEE Transactions on Neural Systems and Rehabilitation Engineering, 2007. **15**(3): p. 379-386.
4. Banala, S.K., S.K. Agrawal, and J.P. Scholz. *Active Leg Exoskeleton (ALEX) for gait rehabilitation of motor-impaired patients*. in *2007 IEEE 10th International Conference on Rehabilitation Robotics, ICORR'07*. 2007.
5. Hesse, S., D. Uhlenbrock, and T. Sarkodie-Gyan, *Gait pattern of severely disabled hemiparetic subjects on a new controlled gait trainer as compared to assisted treadmill walking with partial body weight support.* Clinical Rehabilitation, 1999. **13**(5): p. 401-410.
6. Wheeler, J.W., H.I. Krebs, and N. Hogan. *An ankle robot for a modular gait rehabilitation system*. in *2004 IEEE/RSJ International Conference on Intelligent Robots and Systems (IROS)*. 2004.
7. Montagner, A., et al. *A pilot clinical study on robotic assisted rehabilitation in VR with an arm exoskeleton device*. in *2007 Virtual Rehabilitation, IWVR*. 2007.
8. Wisneski, K.J. and M.J. Johnson, *Quantifying kinematics of purposeful movements to real, imagined, or absent functional objects: Implications for modelling trajectories for robot-assisted ADL tasks.* Journal of NeuroEngineering and Rehabilitation, 2007. **4**.
9. Aoyagi, D., et al., *A robot and control algorithm that can synchronously assist in naturalistic motion during body-weight-supported gait training following neurologic injury.* IEEE Transactions on Neural Systems and Rehabilitation Engineering, 2007. **15**(3): p. 387-400.
10. Riener, R., et al., *Patient-cooperative strategies for robot-aided treadmill training: First experimental results.* IEEE Transactions on Neural Systems and Rehabilitation Engineering, 2005. **13**(3): p. 380-394.
11. Vallery, H., et al., *Reference trajectory generation for rehabilitation robots: Complementary limb motion estimation.* IEEE Transactions on Neural Systems and Rehabilitation Engineering, 2009. **17**(1): p. 23-30.
12. Verdaasdonk, B.W., H.F.J.M. Koopman, and F.C.T. Van Der Helm, *Energy efficient walking with central pattern generators: From passive dynamic walking to biologically inspired control.* Biological Cybernetics, 2009. **101**(1): p. 49-61.
13. Low, K., et al., *Locomotive control of a wearable lower exoskeleton for walking enhancement.* Journal of Vibration and Control, 2006. **12**(12): p. 1311.
14. *https://mindwalker-project.eu/*.
15. Van der Kooij, H., et al., *An alternative approach to synthesizing bipedal walking.* Biological Cybernetics, 2003. **88**(1): p. 46-59.
16. Hof, A., *The 'extrapolated center of mass' concept suggests a simple control of balance in walking.* Human movement science, 2008. **27**(1): p. 112-125.
17. Hurmuzlu, Y., F. Genot, and B. Brogliato, *Modeling, stability and control of biped robots - A general framework.* Automatica, 2004. **40**(10): p. 1647-1664.
18. Diehl, M., H.J. Ferreau, and N. Haverbeke, *Efficient numerical methods for nonlinear MPC and moving horizon estimation*, in *Lecture Notes in Control and Information Sciences*. 2009. p. 391-417.
19. Logist, F., et al., *Fast Pareto set generation for nonlinear optimal control problems with multiple objectives.* Structural and Multidisciplinary Optimization. **42**(4): p. 591-603.
20. Wieber, P.B. *Trajectory free linear model predictive control for stable walking in the presence of strong perturbations*. in *Proceedings of the 2006 6th IEEE-RAS International Conference on Humanoid Robots, HUMANOIDS*. 2006.
21. Ng, A.Y., et al., *Autonomous inverted helicopter flight via reinforcement earning*, in *Springer Tracts in Advanced Robotics*. 2006. p. 363-372.
22. Koopman, B., E.H.F. Van Asseldonk, and H. Van Der Kooij. *In vivo measurement of human knee and hip dynamics using MIMO system identification*. in *2010 Annual International Conference of the IEEE Engineering in Medicine and Biology Society, EMBC'10*.